

The Birth and Death of Toxins with Distinct Functions: A Case Study in the Sea Anemone *Nematostella*

Maria Y. Sachkova,^{*,†,‡,1} Shir A. Singer,^{†,1} Jason Macrander,^{§,2} Adam M. Reitzel,² Steve Peigneur,³ Jan Tytgat,³ and Yehu Moran^{*,1}

¹Department of Ecology, Evolution and Behavior, Alexander Silberman Institute of Life Sciences, Faculty of Science, The Hebrew University of Jerusalem, Jerusalem, Israel

²Department of Biology, University of North Carolina at Charlotte, Charlotte, NC

³Department of Toxicology and Pharmacology, Catholic University of Leuven, Leuven, Belgium

***Corresponding authors:** E-mails: mariasachkova@gmail.com; yehu.moran@mail.huji.ac.il.

[†]These authors contributed equally to the work.

[‡]Present address: Sars International Centre for Marine Molecular Biology, University of Bergen, Bergen, Norway

[§]Present address: Florida Southern College, Lakeland, FL

Associate editor: Mary O'Connell

Novel toxin transcripts were submitted to GenBank under accessions MK608361–MK608362 and MK912031–MK912036. Novel proteomics data were submitted to the ProteomeXchange database under identifier PXD012719.

Abstract

The cnidarian *Nematostella vectensis* has become an established lab model, providing unique opportunities for venom evolution research. The *Nematostella* venom system is multimodal: involving both nematocytes and ectodermal gland cells, which produce a toxin mixture whose composition changes throughout the life cycle. Additionally, their modes of interaction with predators and prey vary between eggs, larvae, and adults, which is likely shaped by the dynamics of the venom system.

Nv1 is a major component of adult venom, with activity against arthropods (through specific inhibition of sodium channel inactivation) and fish. Nv1 is encoded by a cluster of at least 12 nearly identical genes that were proposed to be undergoing concerted evolution. Surprisingly, we found that *Nematostella* venom includes several Nv1 paralogs escaping a pattern of general concerted evolution, despite belonging to the Nv1-like family. Here, we show two of these new toxins, Nv4 and Nv5, are lethal for zebrafish larvae but harmless to arthropods, unlike Nv1. Furthermore, unlike Nv1, the newly identified toxins are expressed in early life stages. Using transgenesis and immunostaining, we demonstrate that Nv4 and Nv5 are localized to ectodermal gland cells in larvae.

The evolution of Nv4 and Nv5 can be described either as neofunctionalization or as subfunctionalization. Additionally, the Nv1-like family includes several pseudogenes being an example of nonfunctionalization and venom evolution through birth-and-death mechanism. Our findings reveal the evolutionary history for a toxin radiation and point toward the ecological function of the novel toxins constituting a complex cnidarian venom.

Key words: birth-and-death evolution, concerted evolution, venom, toxin, Cnidaria, *Nematostella vectensis*, neofunctionalization.

Introduction

The starlet sea anemone *Nematostella vectensis* inhabits brackish lagoons along the east and west coasts of the United States and Canada (Hand and Uhlinger 1992; Darling et al. 2005). During its complex life cycle, *Nematostella* goes through a mobile larval stage (planula) followed by metamorphosis into a sessile adult polyp. Polyps burrow into loose substrate, where they reside with their venom charged tentacles exposed. Females produce eggs loaded into gelatinous packages, whereas males emit sperm into the water. After fertilization, embryos develop inside the egg package until they reach the planula stage (~3 days post fertilization [dpf]), start swimming, and leave the gelatinous package (Hand and Uhlinger 1992). Around 6 dpf, planulae begin metamorphosis into a primary

polyps, distinguished by growing four tentacles around their mouth and settling down on the bottom of the pond. In ~4 months under lab conditions, polyps reach sexual maturity (Hand and Uhlinger 1992). The planula and the adult polyp are considerably different in their morphology (body plan, size) and physiology (the planula is not feeding and motile, whereas the polyp is feeding and sessile), resulting in different interactions with potential predators and prey (Columbus-Shenkar et al. 2018). It is likely that these interactions are mediated by venom and its dynamic composition changes across the life cycle. For example, the toxin NvePtx1 protects eggs and planulae from fish predators, whereas Nv1 toxin is involved in both predation and defense in adults (Columbus-Shenkar et al. 2018).

© The Author(s) 2019. Published by Oxford University Press on behalf of the Society for Molecular Biology and Evolution.

This is an Open Access article distributed under the terms of the Creative Commons Attribution License (<http://creativecommons.org/licenses/by/4.0/>), which permits unrestricted reuse, distribution, and reproduction in any medium, provided the original work is properly cited.

Open Access

The *Nematostella* venom system is quite complex. Both polyps and planulae are equipped with two types of venom producing cells: stinging cells (nematocytes) and gland cells with different toxins (Moran et al. 2012, 2013). For example, ectodermal gland cells produce NvePtx1 in planulae and Nv1 in adults, whereas nematocytes are charged with NEP3 toxin throughout multiple stages of the *Nematostella* life cycle (Columbus-Shenkar et al. 2018).

Nv1 is the major component of adult venom (Moran et al. 2012). It is highly selective to arthropod sodium channels and acts through inhibition of their inactivation (Moran, Weinberger, Reitzel, et al. 2008). Exposure to Nv1 toxin leads to contraction paralysis in arthropods, which under native conditions might be either prey (e.g., copepods [Frank and Bleakney 1978]) or predators (grass shrimps [Kneib 1985]). Remarkably, Nv1 is encoded by a cluster of at least 12 nearly identical genes that were proposed to be undergoing concerted evolution (Moran, Weinberger, Sullivan, et al. 2008). Similar ultraconservation of toxin genes likely due to concerted evolution was also reported in other sea anemones, *Actinia equina* and *Anemonia viridis*, suggesting that this mechanism is common for toxin genes of sea anemones (Moran et al. 2009). However, some of the toxin paralogs in *Actinia* and *Anemonia* also exhibited high sequence diversity, suggesting they escaped concerted evolution, instead evolving under positive selection. The fact that members of each group of paralogous toxins in each species is more similar to one another than to their homologs in the other species is a strong indication for concerted evolution (Moran, Weinberger, Sullivan, et al. 2008). Generally, concerted evolution is considered to be a very rare evolutionary pattern, and even when it is observed in most cases it is usually short lived (Nei and Rooney 2005; Sugino and Innan 2006). However, there are also opposing views regarding the lifetime of concerted evolution based on the recent discovery of long-lasting sequence conservation of duplicated genes in prokaryotes (Wang and Chen 2018).

In most other animals, venom genes are hypothesized to evolve mostly via birth-and-death evolution, which is considered to be the common evolutionary pattern of protein-coding gene families in general (Fry et al. 2003; Nei and Rooney 2005; Casewell et al. 2013). This general expectation raises the intriguing question why sea anemone sodium channel toxins exhibit such an unusual evolutionary trajectory following their duplication, and whether this is true for all members of this gene family or if some paralogs escape concerted evolution as in *Actinia* and *Anemonia*.

In this work, we found that *Nematostella* venom includes several Nv1 paralogs that have escaped concerted evolution. Because *Nematostella* has become a lab model with established genetic tools, we were able to dissect the dynamic expression patterns of the newly identified genes. Additionally, we used toxicity assays and pharmacology to characterize the new toxins. Our findings reveal the evolutionary history and point toward the ecological function of the new toxins and further reveal the complexity of the venom of *Nematostella*.

Results

Nv1 Homologs Escaping Concerted Evolution

Using BLAST searches in the *Nematostella* transcriptome, we found several sequences encoding precursor proteins homologous to Nv1 toxin. They were named as Nv4, Nv5, Nv6, Nv7, and Nv8 (altogether the Nv1-like family) (fig. 1A). The sequences were highly divergent, with identity to Nv1 ranging between 26% and 33% for most of the novel sequences, with identity to each other not exceeding 64% (fig. 1A and supplementary table 1, Supplementary Material online). Regardless of the low sequence similarity, genes encoding Nv1-like proteins had conserved structure (fig. 1B). Their coding sequences consisted of two exons separated by a phase 1 intron. The encoded proteins have domain structure typical of sea anemone toxin precursors (Anderluh et al. 2000), consisting of a signal peptide (identified by SignalP online tool) followed a propeptide and a processing motif upstream a mature peptide with a 6-cysteine motif (Honma and Shiomi 2006; Moran et al. 2009). In all of the proteins except one, the processing motif was represented by a dibasic sequence Lys-Arg. The predicted processing motif for Nv6 most likely corresponds to Asp-Pro sequence recently reported in *Metridium senile* (Logashina et al. 2017).

Type I and Type II sea anemone toxins share the same rare pattern of cysteines (CXC-C-C-CC, where X is any residue apart from cysteine), which until now has not been reported in the toxins of other animals (Mouhat et al. 2004; Moran et al. 2009). The Nv1 toxin is known to share similarity to Type I and Type II sea anemone toxins (Moran and Gurevitz 2006; Moran, Weinberger, Reitzel, et al. 2008). Among the members of Nv1-like family, Nv1 has the highest identity with Av2 (Type I toxin from *Anemonia viridis*) and Sh1 (Type II toxin from *Stichodactyla helianthus*). On the other hand, Nv4, Nv5, Nv6, and Nv7 were more similar to Nv1 than to Sh1 and Av2 (fig. 1A). This suggests that the newly discovered Nv1 homologs might have resulted from gene duplications specific to the Edwardsiidae (the taxonomic family to which *Nematostella* belongs) of an Nv1-like ancestor followed by diversification.

Anthozoan Type III potassium channel neurotoxins share the same cysteine pattern as Type I and Type II sodium channel neurotoxins and were suggested to have evolved from them (Jouiaei et al. 2015). To study the evolutionary history of the Nv1-like peptides, we created a list of sequences including precursors of characterized and putative anthozoan toxins sharing this rare cysteine pattern (supplementary file 1, Supplementary Material online). We attempted to reconstruct their phylogeny with methods such as maximum likelihood and Bayesian inference, however due to their short sequence length and high rates of substitutions these analyses resulted in very low branch support values (supplementary fig. 3, Supplementary Material online). Therefore, we used an alternative clustering analysis, the CLuster ANalysis of Sequences (CLANS) software (Frickey and Lupas 2004), which uses pairwise comparisons and was shown to be effective for short and highly diverse sequences such as neuropeptides

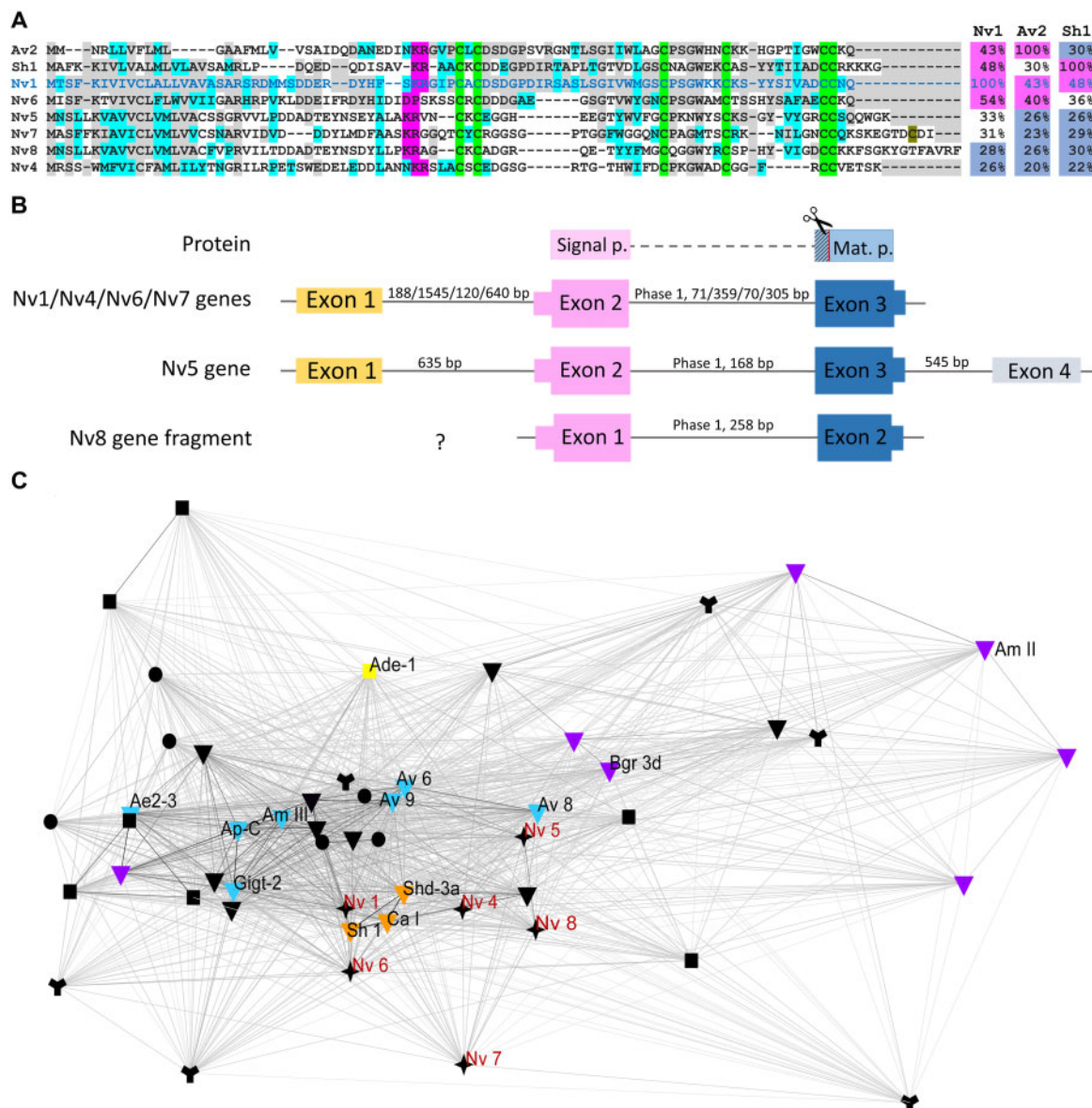


Fig. 1. Evolution of Nv1 homologs. (A) Alignment of Nv1 precursor to newly identified homologs from *Nematostella* (Nv4, Nv5, Nv6, Nv7, Nv8) and to the Type I toxin Av2 from *Anemonia viridis* and the Type II toxin Sh1 from *Stichodactyla helianthus*. Identical and conserved residues are highlighted in gray and blue, respectively. Cysteine residues making part of the disulfide framework are in green; note that Nv7 has one additional cysteine residue highlighted in olive. Processing site is in purple. Percentage of identity to Nv1, Av2, and Sh1 are shown at the right; values in the range of 0–30% are in blue, 40–100% are in pink. (B) Gene structure is conserved throughout all the Nv1 homologs in *Nematostella*; only Nv5 has additional exon in its 3' UTR. Annotation of the coding regions is according to the publicly available gene models (David Fredman; Michaela Schwaiger; Fabian Rentzsch; Ulrich Technau [2013]; *Nematostella vectensis* transcriptome and gene models v2.0. figshare. Data set; <https://doi.org/10.6084/m9.figshare.807696.v1>; Last accessed on June 1, 2019). For Nv8, manual alignment of transcripts to genome scaffold was performed. Numbers indicate intron length in the same order as the names of the genes. UTRs are represented by narrower rectangles, whereas coding sequences are shown by wider rectangles. The gene structures are aligned to the protein precursor structure; Signal p., signal peptide; Mat. p., mature peptide, propeptide is designated by the diagonal pattern, the processing site is indicated by the scissors and red line. (C) Clustering of Nv1 and newly identified homologs from *Nematostella* with homologs from other anthozoan species by the CLANS software. Sequences from *Nematostella* are shown as stars, other Edwardsioidea—as a bold Y-shape, Actinioidea sequences are represented by triangles, Metridioidea—by squares, and stony corals—by circles (classification by Rodriguez et al. [2014]). Blue represents Type I sodium channel toxins, orange—Type II sodium channel toxins, purple—Type III potassium channel toxins (sequences designated as toxins only by homology are also included). Names are shown for characterized toxins. Edges represent BLAST high scoring segment pairs (HSPs) and their thickness corresponds to attraction forces proportional to the negative logarithm of the HSP's P values ($10^{-1} < P < 10^{-48}$).

(Jekely 2013). Similarly to Nv1, the CLANS analysis showed that all the new Nv1-like sequences were similar to Type I and Type II toxin sequences (fig. 1C) (Jouiaei et al. 2015).

Apart from the sequences encoding full open reading frames, we also retrieved three sequences from both the transcriptome and genome encoding homologs of Nv1 family

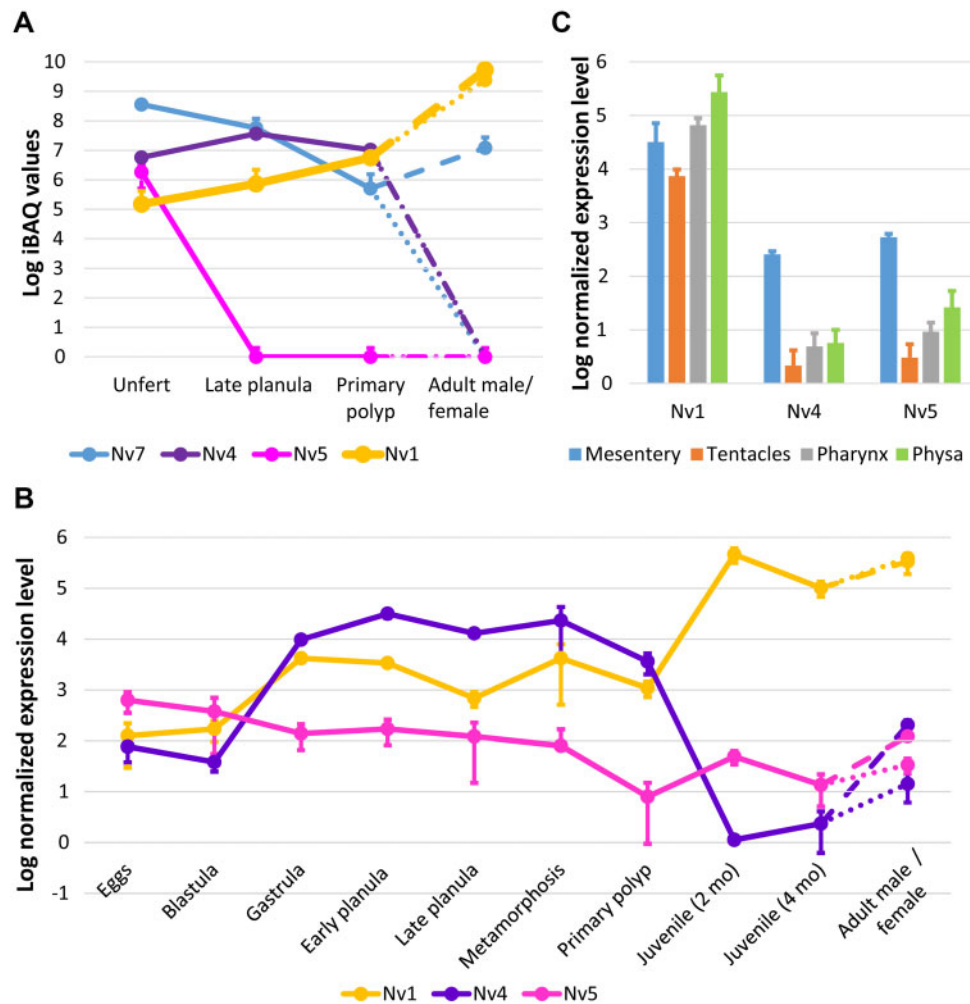


Fig. 2. Spatiotemporal dynamics of expression among Nv1 homologs. (A) Proteomic dynamics of Nv1-like peptides measured by LC-MS/MS. (B) Transcriptional dynamics of Nv4 and Nv5 measured by nCounter platform. (C) Transcription levels of Nv4 and Nv5 in adult female tissues. In all the three plots (A–C) error bars represent standard deviations. In the panels A and B, values for adult females are shown with dash lines, and for adult males—with dotted lines. Values for Nv1 are from Columbus-Shenkar et al. (2018) apart from the eggs stage at panel A that was measured in the current work.

peptides interrupted by premature stop codons, which indicate they are most probably pseudogenes (supplementary fig. 1, Supplementary Material online). Pseudogene 1 is highly similar to Nv8 and represented by two gene copies, one of which resides on the same gene scaffold as Nv8. Pseudogene 2 appears to result from a duplication of the last coding exon of Nv8. The sequence of pseudogene 3 is highly divergent from other Nv1-like sequences and is interrupted by two premature stop codons. This third locus might have evolved by a duplication of the last coding exon of one of the Nv1 family members. Additionally, we found a full Nv1-like open reading frame missing one cysteine residue of the otherwise conserved pattern; we named it Nv-mut.

Nv1 is encoded by multiple gene copies residing in the same locus and undergoing concerted evolution (Moran, Weinberger, Sullivan, et al. 2008). The high sequence divergence of the new Nv1-like homologs suggests that, unlike Nv1, they have been escaping concerted evolution. Importantly, all the Nv1-like genes are localized on genomic scaffolds different from the multiple Nv1 gene copies

(according to the publicly available gene models [David Fredman; Michaela Schwaiger; Fabian Rentzsch; Ulrich Technau {2013}]). The significant distance from Nv1 cluster might explain how Nv1-like genes escaped concerted evolution and why they are highly divergent.

Analysis of Spatiotemporal Expression Dynamics

Recently, we and others have shown that sea anemones express different toxins at distinct developmental stages and tissues (Moran et al. 2013; Macrander et al. 2016; Columbus-Shenkar et al. 2018; Surm et al. 2019). To explore the expression dynamics of the newly discovered genes, we analyzed previously published data sets as well as proteomic measurements we performed as part of the current study. We identified Nv1, Nv4, Nv5, and Nv7 in proteomes of *Nematostella* derived from different developmental stages (fig. 2A). Nv6 and Nv8 were not detected by LC-MS/MS at any developmental stage, probably due to low expression levels. According to the proteomics data, Nv4, Nv5, and Nv7 are detectable in unfertilized eggs. The expression

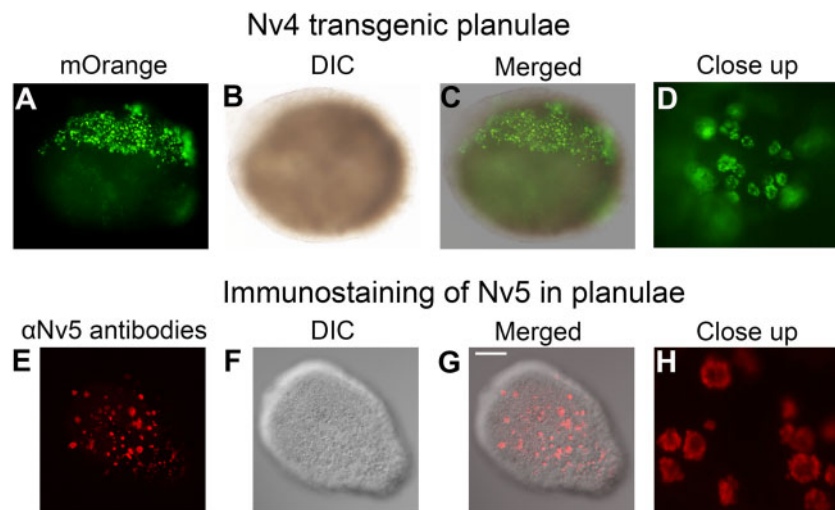


Fig. 3. Nv4 and Nv5 are localized in ectodermal gland cells of *Nematostella* planulae. (A–C) Transgenic planulae expressing memOrange2 under control of Nv4 promoter. memOrange2 is localized in ectodermal cells. (D) In transgenic planulae, memOrange2 is driven into vesicles probably due to the fusion to Nv4 signal peptide. (E–G) Immunostaining of Nv5 in wild type planulae.

pattern of Nv7 was remarkably similar to the expression pattern of NvPt1, a defensive toxin found in the stages from eggs to primary polyps and adult females (fig. 2A) (Columbus-Shenkar et al. 2018). Nv4 is expressed until the primary polyp stage, whereas Nv5 is present only in the eggs.

At the transcriptomic level, Nv1, Nv4, Nv5, Nv6, and Nv7 were found in an embryogenesis transcriptome database which includes stages from unfertilized eggs to primary polyp (supplementary fig. 2, Supplementary Material online) (Fischer et al. 2014; Warner et al. 2018). In early stages, Nv4, Nv5 and Nv7 are expressed at higher levels and expression decreases by primary polyp stage. Some of our findings were also supported by the single cell transcriptome data (Sebe-Pedros et al. 2018), with Nv4 and Nv7 found among genes expressed at the planula larval stage. For further assays, we chose to focus on Nv4 and Nv5, whose expression pattern appeared to be drastically different from Nv1. Another reason for this choice was the fact that Nv4 and Nv5 have a higher potential for functional characterization compared with Nv7, which has an uneven number of cysteine residues in its mature sequence (fig. 1A), a feature that can hinder recombinant production.

To dissect in greater detail the expression patterns of Nv4 and Nv5, we measured their expression at the mRNA level by nCounter technology at multiple developmental stages: unfertilized eggs, blastulae, gastrulae, early planulae (2 dpf), planulae (4 dpf), metamorphosing planulae (6 dpf), primary polyps (10 dpf), juvenile polyps (2 and 4 months old), adult males, and adult females (fig. 2B). The highest expression level of Nv5 was observed in the unfertilized eggs. Starting from blastula stage, it gradually drops till the metamorphosis stage and peaks again in the adult females. Nv4 is expressed at the highest level from blastula to the primary polyp stage and it can be detected in adult females as well. Nv1 genes are expressed in all the life stages of *Nematostella*, however, starting from the juvenile polyp their expression increases

by at least two orders of magnitude (Columbus-Shenkar et al. 2018). Importantly, Nv1 is not translated until after the larval stage due to intron retention (Moran, Weinberger, Reitzel, et al. 2008) and therefore Nv1 can be considered purely an adult toxin.

nCounter measurements in different tissues of adult females (fig. 2C) showed that expression of Nv4 and Nv5 is much higher ($20\text{--}176$ times, $P < 5.1 \times 10^{-4}$, Student's *t*-test) in mesenteries than in tentacles, pharynx, and physa. Mesentery is the tissue producing gametes and therefore the high expression of Nv4 and Nv5 might indicate that they are maternally deposited into eggs, similarly to NvPt1 (Columbus-Shenkar et al. 2018). In contrast to Nv4 and Nv5, Nv1 did not show elevated expression level in the mesenteries: differences with the other tissues are in the range between 0.1 and 4 and are not statistically significant (Student's *t*-test, $P > 0.2$).

Localization of Nv4 and Nv5 Expression

To dissect the spatial expression pattern of Nv4 at the cellular level, we generated a transgenic construct to be injected into zygotes. We amplified a genomic fragment including 660-bp upstream of exon 1 followed by exon 1, intron 1, exon 2, and intron 2 and a fragment of exon 3 encoding a part of propeptide up to the processing site (for gene structure see fig. 1B). We anticipated that this genomic fragment will include a promoter and regulatory regions in addition to the fragment of the sequence coding for signal peptide and propeptide. The fragment was cloned into a vector upstream of a sequence encoding memOrange2, a fluorescent protein (Shaner et al. 2008). Thus, we generated an artificial gene whose product was a fusion between the fluorescent protein and Nv4 prepropeptide facilitating its cotranslational transport to the endoplasmic reticulum. Expression of this new product was under control of the Nv4 regulatory region. Thus, the

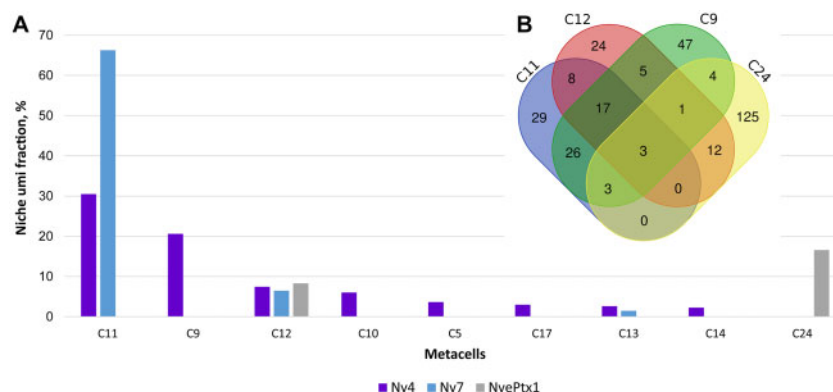


FIG. 4. Different types of ectodermal gland cells produce venom components in *Nematostella* larvae according to single cell RNAseq data analyses (Sebe-Pedros et al. 2018). (A) Distribution of Nv4, Nv7, and NvePtx1 expression between different larval metacells. (B) Venn diagram of genes expressed in C9, C11, C12, and C24, the metacells engaged the most into toxin production. Only three genes are shared between all the four metacells. The diagram was created using DrawVennDiagram online tool (<http://bioinformatics.psb.ugent.be/webtools/Venn/>; Last accessed on June 1, 2019).

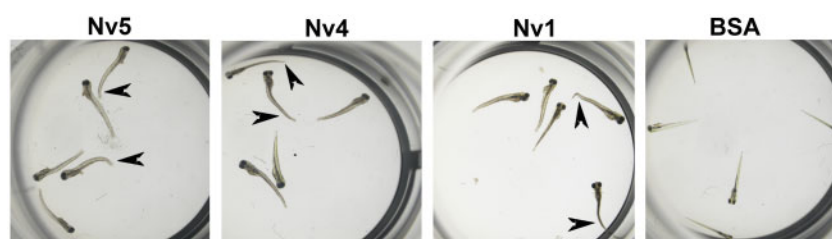


FIG. 5. Toxicity tests of Nv4, Nv5, Nv1, and BSA (negative control) on zebrafish larvae. Abnormally bent and contracted tails due to toxic effects are indicated by arrowheads.

memOrange2 expression pattern and intracellular localization should mimic the native expression of Nv4.

The expression of the Nv4 transgenic construct was first detected in the early embryos and the memOrange2 fluorescent marker was localized to the ectodermal cells of planulae. Further, the fluorescent protein was localized in the cytoplasmic vesicles (fig. 3A–D) indicating that Nv4 is produced and secreted by ectodermal gland cells. By the primary polyp stage, expression disappeared. This pattern of expression was similar to the patterns observed by our nCounter and proteomics data.

To study Nv5 localization, we used immunostaining in planulae with anti-Nv5 antibodies. The staining was observed in ectodermal gland cells (fig. 3E–H). Thus, both Nv4 and Nv5 are secreted by planula ectodermal cells and indeed might be venom components. Strikingly, the gland cells producing Nv4 and Nv5 are very different in size meaning that different types of gland cells are specialized on the production of these peptides.

In the single cell, RNAseq study on *Nematostella* larvae and polyps, Sebe-Pedros and coauthors (Sebe-Pedros et al. 2018) grouped individual cells with highly similar expression profiles based on a statistical cutoff into “metacells” representing various cell states or cell types. Nv4, Nv7, and NvePtx1 are expressed in planula, whereas Nv5 was not identified, probably due to lower expression level (at the planula stage, the difference between expression levels of Nv4 and Nv5 is at least two orders of magnitude, see fig. 2B). All three genes are

coexpressed in the C12 metacell, whereas C11 and C13 metacells coexpress Nv4 and Nv7 (fig. 4A). In the planula, cells producing Nv4 and NvePtx1 are ectodermal gland cells and hence we conclude that Nv7 is expressed in ectodermal gland cells as well. Additionally, Nv4 was detected in the C5, C9, C10, C14, and C17 metacells, whereas NvePtx1 was identified in the C24 metacell. Expression levels of the peptides vary significantly between the metacells, with C11 and C9 metacells accounting for 51% of total Nv4 expression, C11 accounts for 66% of Nv7 expression, and C24 for 16% of NvePtx1 expression. We compared sets of genes upregulated in larval metacells with the most toxin production: C11 (86 genes), C9 (106 genes), C24 (148 genes), and C12 (70 genes) (fig. 4B). Surprisingly, only three genes are upregulated in all the four metacells: v1g242983 (unknown secreted protein, similar to Collagen alpha-1[XII] chain from *Stylophora pistillata*), v1g245153 (unknown secreted protein), and v1g237037 (Tetraspanin). These data indicate that planulae possess different types of ectodermal gland cells differing considerably in the kinds and number of toxins they produce.

Functional Characterization

To enable the testing of their potential toxicity, Nv4 and Nv5 were produced in recombinant form in *Escherichia coli* and purified by a two-step chromatographic procedure. To assay the toxicity of Nv4 and Nv5 in comparison to Nv1, we incubated zebrafish larvae ($N = 10$) in 0.5 mg/ml solution of the

recombinant peptides in parallel to a bovine serum albumin (BSA) control (5 mg/ml). Nv5 caused death of all the fishes within 30 min, Nv4 within 40 min, and Nv1 within 1 h. Toxic effects, particularly contractile paralysis accompanied by twitching of the tail, began within 20 min for Nv5 and 30 min for Nv4 (fig. 5 and supplementary videos 1 and 2, Supplementary Material online). All the larvae incubated with BSA survived. The experiment was performed twice.

Additionally, we tested activity of Nv4 and Nv5 on cherry shrimps by injecting peptides at a dose of 1 µg/100 mg body weight in parallel with Nv1. Both Nv4 and Nv5 did not show any effect, whereas Nv1 paralyzed shrimps immediately after injection in doses at least ten times lower. Experiments with native *Nematostella* predators, grass shrimps (*Palaemonetes* sp.), showed similar results: 5/5 animals injected with Nv4 or Nv5 at a dose of 25 ng/100 mg body weight survived, whereas Nv1 was lethal at the same concentration (reported LD₅₀ for Nv1 is 1.25 ng/100 mg shrimp [Columbus-Shenkar et al. 2018]).

Electrophysiological assays (supplementary fig. 4, Supplementary Material online) showed that Nv4 and Nv5 did not have any effect on mammalian (hNa_v1.1, rNa_v1.2, rNa_v1.3, rNa_v1.4, hNa_v1.5, mNa_v1.6, rNa_v1.8) and insect (BgNa_v1) voltage-gated sodium channels, whereas Nv1 selectively inhibited inactivation of BgNa_v1 (similarly to the effect on *Drosophila* DmNav1 channel [Moran, Weinberger, Reitzel, et al. 2008]). In the tests on a large variety of voltage-gated potassium channels (rKv1.1, rKv1.2, hKv1.3, rKv1.4, rKv1.5, rKv1.6, *Drosophila* Shaker IR, rKv2.1, hKv3.1, rKv4.3, hKv7.2, hKv7.3, hKv10.1 and the human Ether-à-go-go-Related Gene [hERG]), all three toxins did not have any effect. These results suggest that Nv4 and Nv5 do not target vertebrate voltage-gated sodium and potassium channels and probably interfere with activity of another receptor in zebrafish. Activity pattern on arthropod ion channels is consistent with toxicity pattern on shrimps: Nv1 but not Nv4 and Nv5 was specifically active on arthropod sodium channel.

Discussion

Our study shows that Nv4 and Nv5, similarly to Nv1, are venom components produced by ectodermal gland cells. These three highly divergent toxins are a result of gene duplications followed by significant diversification in their temporal and spatial expression patterns as well as their function on potential prey and predators. Unlike Nv1, which is found in polyps, Nv4 and Nv5 are produced in early developmental stages of *Nematostella*. Because *Nematostella* does not feed until the primary polyp stage, toxins such as Nv4 and Nv5 produced only from egg to planula stages can be assumed to play purely a protective role. The protective roles of some toxins was also shown in cone snails, which inject different venoms in predatory and defensive scenarios (Dutertre et al. 2014) and also in assassin bugs that can utilize different venom glands (Walker et al. 2018). This functional convergence in the venom systems of mollusks, insects, and cnidarians suggest that there is an advantage in separating defensive and offensive venoms. Nv4 and Nv5 are lethal for zebrafish larvae, but not to shrimps, indicating that they

might have evolved under selective pressure from natural fish predators. As it was previously shown (Columbus-Shenkar et al. 2018), larvae of the killifish *Fundulus heteroclitus*, a possible native predator of *Nematostella*, avoid feeding on eggs and planulae of the anemone. Thus, Nv4 and Nv5 along with other larval venom components such as NvPt1 and NEP3 contribute to the resistance toward fish predators in the larval stage. On the other hand, grass shrimps are able to feed on both egg packages and individual eggs (Columbus-Shenkar et al. 2018), which correlates a lack of toxicity of both Nv4 and Nv5 as well as NvPt1 and NEP3 for shrimp. In adults, Nv1 might be involved in predation on arthropods and defense against them. According to the single cell transcriptome data (Sebe-Pedros et al. 2018), Nv7 is coexpressed with other toxins in the planula gland cells indicating that it might also be a venom component.

Among all the members of the Nv1-like family, Nv1 shares the highest sequence identity with Av2 and Sh1 toxins produced by different sea anemone species. This similarity suggests that the last common ancestor of Nv1-like family might have been more similar to Nv1 rather than to other members of the family and Nv4, Nv5, Nv6, Nv7, and Nv8 might have resulted from Edwardsiidae-specific gene duplications.

Multiple gene copies encoding Nv1 undergo concerted evolution via gene conversion or unequal crossing over (Moran, Weinberger, Sullivan, et al. 2008). Genomic proximity between the gene copies is one of the factors enhancing the rate of concerted evolution (Liao 1999). Therefore, the translocation of the Nv1 paralogs to different loci may have resulted in them escaping concerted evolution and diverging in evolutionary trajectories from Nv1. A similar scenario was proposed for translocated insect ribosomal RNA genes that show unusually high heterogeneity (Keller et al. 2006) unlike the vast majority of such genes in eukaryotes that are typified by homogeneity (Eickbush and Eickbush 2007). The translocation of Nv4, Nv5, and Nv7 changed their genomic environment and probably contributed to evolution of new regulatory elements and different expression dynamics. Nv1 genes are expressed in all the developmental stages (even though from embryo to planula stages translation does not happen due to intron retention [Moran, Weinberger, Reitzel, et al. 2008]), whereas Nv4 and Nv5 expression decreases after the planula stage (fig. 2). If the Nv1 expression profile resembles the ancestral condition, we could hypothesize that the regulatory mechanism activating expression of Nv4 and Nv5 in adult tissues (apart of the female mesenteries) was lost after the translocation. Proteomics and immunostaining confirmed that Nv4 and Nv5 were produced at protein level in early life cycle stages and thus lost regulation by intron retention as well. This scenario can be described as neofunctionalization: acquisition of new expression pattern and purely protective function (fig. 6). The change of function is also clear based on their different pharmacological profiles (supplementary fig. 4, Supplementary Material online) and effects on vertebrate predators, where Nv4 and Nv5 are highly toxic for fish, whereas Nv1 combines strong arthropod with weaker fish toxicity. Previous bona fide cases of neofunctionalization in enzymes and transcription factors were shown to involve

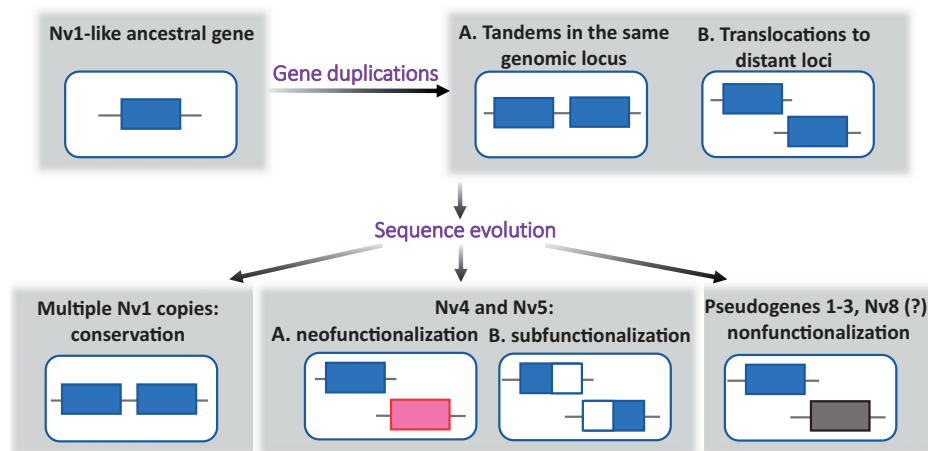


Fig. 6. Summary of the possible evolutionary scenarios of the origin of the Nv1-like family.

differences in activities and spatiotemporal expression patterns of paralogs, similarly to the case we describe here for these neurotoxins (Zhang et al. 2002; Chen et al. 2012). We can alternatively hypothesize that the last common ancestor of the Nv1-like family possessed both anti-fish and anti-arthropod functions and was expressed in all developmental stages. In this scenario, during the course of evolution Nv4 and Nv5 underwent subfunctionalization by specializing on anti-fish toxicity and expression in young life stages whereas Nv1 specialized in anti-arthropod activity in the adult polyp stage (fig. 6).

Some of the copies of the Nv1-like gene family have undergone nonfunctionalization due to nonsense mutations resulting in at least three pseudogenes interrupted by premature stop codons and Nv8 with negligible expression level. The evolution of these members of the Nv1-like family is a clear example for venom evolution through birth-and-death mechanism (Nei and Rooney 2005). This evolutionary mode has been hypothesized multiple times in various venomous animals (Casewell et al. 2013; Casewell 2016), but “gene death” has only rarely been demonstrated (Chijiwa et al. 2000; Dowell et al. 2016). Further, our results show that both birth and death and concerted modes of evolution can coexist in the same gene family and are not necessarily opposing each other as previously hypothesized (Nei and Rooney 2005).

Transgenesis and immunostaining experiments showed that Nv4 and Nv5 are produced by different types of gland cells that differ in size (fig. 3A–H). In our previous work (Columbus-Shenkar et al. 2018), we showed that NvePtx1 is expressed in two types of gland cells differing in size as well. Single cell RNAseq data showed that Nv4, Nv7, and NvePtx1 are expressed by different metacells, which might represent either different types of cells or different transcription states. Multiple types of venom producing gland cells, similarly to diverse nematocyte types (Columbus-Shenkar et al. 2018), may provide a cellular context for dynamic regulation of venom production in planulae and higher flexibility in relatively short evolutionary times. This can be attained by the increased modularity achieved by multiple types of gland cells expressing different venom cocktails.

Materials and Methods

Alignment, Clustering, and Phylogenetic Reconstruction

To align Nv1 to its homologs from *Nematostella*, Clustal Omega was used (<https://www.ebi.ac.uk/Tools/msa/clustalo/>). Last accessed on June 1, 2019

Sequences of Nv1, Nv4, Nv5, Nv6, and Nv8 precursors were used for BLAST searches (<https://blast.ncbi.nlm.nih.gov/Blast.cgi>; Last accessed on June 1, 2019) in NCBI databases (Nucleotide collection, Transcriptome Shotgun Assembly, nonredundant protein sequences). Searches for sequences with similarity to the Nv1-like family were also conducted in EdwardsiellaBase (Stefanik et al. 2014), Compagen (Hemrich and Bosch 2008), and Reefgenomics (Liew et al. 2016) databases as well as an in-house *Exaipiasia pallida* and *Edwardsia elegans* transcriptomes. All searches were limited to Cnidaria. Nucleotide sequences were translated and amino acid sequences sharing the same cysteine pattern as the query sequences and containing a signal peptide (identified by the SignalP 4.0 [Petersen et al. 2011]) were retained for further analysis. In total, 331 protein sequences were retrieved. To exclude redundant sequences and multiple highly similar sequences, we clustered the list with a threshold of 80% identity by the CD-HIT online tool (Huang et al. 2010). One sequence from each cluster was randomly chosen to create a final list of 53 protein sequences. The threshold of 80% was chosen because Nv1-like family members do not share more than 50% identity with sequences outside the Edwardsiidae and not more than 65% identity with any available non-*Nematostella* sequence. Therefore clusters of highly similar sequences would not contribute significant information to the phylogenetic analysis and clustering.

For phylogenetic analysis, all the sequences were aligned using MAFFT software, version 7, available online at <https://mafft.cbrc.jp/alignment/server/>; Last accessed on June 1, 2019 (Katoh et al. 2017). Substitution model was identified by ProtTest software, version 3 (Darriba et al. 2011). For maximum likelihood phylogenetic reconstruction, we used the PhyML algorithm (Guindon et al. 2010) either in command line mode or implemented into the SeaView platform version

4.7 (Gouy et al. 2010) with following settings: start with BioNJ tree, 100 bootstraps. Bayesian phylogeny was reconstructed with MrBayes version 3.2 (Ronquist et al. 2012) for 3 million generations and the potential scale reduction factor (PSRF) reached 1.000, indicating that the runs converged.

The CLANS software (Frickey and Lupas 2004) was used for clustering analysis with default settings and 1,678,863 rounds.

Nematostella Lab Culture

Adult polyps were cultured in 16‰ artificial sea water (ASW) at 17 °C. Embryos, larvae, and juvenile polyps were kept at 22 °C in the 16‰ ASW. Gamete spawning was induced as previously described (Genikhovich and Technau 2009). Feeding with *Artemia* nauplii was performed three times a week.

Gene Expression

Gene expression analysis was performed as described elsewhere (Columbus-Shenkar et al. 2018). Briefly, total RNA was extracted from different life stages of *Nematostella* as well as different adult female tissues using Tri-Reagent (Sigma-Aldrich, St. Louis, MO). Each sample was prepared in technical replicates and measured using nCounter platform (NanoString Technologies, Seattle, WA; performed by Agentek Ltd., Tel Aviv, Israel). Two specific probes were designed for each gene to hybridize with the respective mRNA and enable measurement of fluorescence intensity of barcodes on one of the probes. Fluorescence intensity is proportional to the concentration of the mRNA. A geometric mean of the expression levels of five reference genes with stable expression across development was used for normalization. Probe sequences as well as all raw and normalized nCounter read data are available in [supplementary table 2](#) and file 2, [Supplementary Material](#) online.

Proteomics

To study temporal dynamics of expression of Nv1 homologs at the protein level, we combined LC-MS/MS data reported earlier (ProteomeXchange identifier PXD008218 [Columbus-Shenkar et al. 2018]) for the late planula, primary polyp, adult males, and females stages with new data for the unfertilized egg stage (ProteomeXchange identifier PXD012719). Here, we used the same unfertilized egg samples as in PXD008218 but ran LC-MS/MS (four replicates) separately from other life stages to eliminate possible crosscontamination with abundant toxins expressed at adult stage. To control for comparability to the older PXD008218 data set, we also reran adult female LC-MS/MS (one replicate). Otherwise, the same experimental and data processing conditions were used as in the earlier study (Columbus-Shenkar et al. 2018).

Transgenesis

To produce a Nv4 transgenic construct, we used plasmids generated in our previous work (Columbus-Shenkar et al. 2018) where *memOrange2* gene was placed under control of the *NEP3* promoter. In this work, *NEP3* regulatory sequences were replaced with a putative Nv4 regulatory sequence. A

genomic fragment (scaffold_75:269319–272282. Coordinates follow [Putnam et al. 2007]), which included the putative promoter, the 5' untranslated region, and the beginning of the coding sequence of the Nv4 gene, was amplified by polymerase chain reaction and cloned into the plasmid upstream *memOrange2* sequence. The transgenic plasmid was injected into fertilized eggs along with the yeast meganuclease I-SceI (New England Biolabs, Ipswich, MA) to facilitate genomic integration following an established protocol (Renfer and Technau 2017). For visualization, 3-day-old transgenic planulae were briefly fixed in 3.7% formaldehyde in 16‰ ASW (20 min, 4 °C) and analyzed under Eclipse Ni-U microscope equipped with a DS-Ri2 camera and an Elements BR software (Nikon, Tokyo, Japan).

Protein Expression and Purification

Synthetic gene fragments encoding Nv4 and Nv5 mature peptides were purchased from Integrated DNA Technologies (Coralville, IA) and cloned into a modified pET40 vector (fragment encoding DSBC signal peptide had been removed [Columbus-Shenkar et al. 2018]) downstream the sequence encoding DSBC. A Tobacco Etch Virus protease cleavage site was introduced between the DSBC and toxin sequences. In the synthetic gene fragments, codon usage was optimized for expression in *E. coli*. Nv4 and Nv5 were expressed in BL21 (DE3) *E. coli* (Merck Millipore, Burlington, MA) as fusion proteins with His₆-DSBC. The polyhistidine tag enabled purification of the fusion proteins from the total *E. coli* lysate by nickel affinity FPLC and cleaved with Tobacco Etch Virus protease (room temperature, overnight). Reverse phase FPLC on a Resource RPC column (GE Healthcare, Uppsala, Sweden) with an acetonitrile concentration gradient in 0.1% trifluoroacetic acid was used to further purify the recombinant toxins. The peptides were vacuum dried and stored at −80 °C.

Immunostaining

Polyclonal rabbit antibodies against Nv5 were purchased from Eurogentec (Liège, Belgium). Prior to immunization, preimmune sera were screened by Western blot and immunostaining to select rabbits with the lowest level of nonspecific antibodies for these *Nematostella* proteins. For immunization, pure recombinant Nv5 was used. Total immunoglobulin was purified using affinity chromatography on a protein G column. Immunostaining on 4 days old planulae was performed according to a published protocol (Moran et al. 2012).

Toxicity Tests

Zebrafish (*Danio rerio*) larvae younger than 120 h were kindly provided by Dr Adi Inbal (The Hebrew University Medical School). The usage of such young larvae does not require ethical permits according to the European and Israeli laws. Five zebrafish larvae (4 dpf) were placed into a 500-μl well and incubated with Nv4, Nv5, and Nv1 at a concentration of 0.5 mg/ml. Toxic effect was monitored under an SMZ18 (Nikon) stereomicroscope during 1 h of incubation. BSA (5

mg/ml) was used as a negative control. Each experiment was performed in duplicate.

Cherry shrimps (*Neocaridina davidi*) were purchased from a local pet store. Toxins were dissolved in PBS buffer and injected in doses of 1 µg/100 mg or 0.1 µg/100 mg of body weight into the shrimp abdomen. Three shrimps were injected at each concentration and every experiment was performed in duplicate. PBS buffer was used as a negative control. Grass shrimps (*Palaemonetes* sp.) were collected at the Belle W. Baruch Institute for Marine and Coastal Sciences (Columbia, SC), transported to the lab and kept in 15‰ ASW until use.

Electrophysiology

For the expression of NaV channels (mammalian hNav1.1, rNav1.2, rNav1.3, rNav1.4, hNav1.5, mNav1.6, rNav1.8 channels, the insect channel BgNaV1 from *Blattella germanica* and the auxiliary subunits β 1, β 2 and TipE) and Kv channels (mammalian rKv1.1, rKv1.2, hKv1.3, rKv1.4, rKv1.5, rKv1.6, rKv2.1, hKv3.1, rKv4.3, hKv7.2, hKv7.3, hKv10.1, the hERG and *Drosophila* Shaker IR) in *Xenopus laevis* oocytes, the linearized plasmids were transcribed using the T7 or SP6 mMESSAGE-mACHINE transcription kit (Ambion, Carlsbad, CA). The harvesting of stage V–VI oocytes from anesthetized female *Xenopus laevis* frog was previously described (Peigneur et al. 2015). Oocytes were injected with 50 nl of cRNA at a concentration of 1 ng/nl using a microinjector (Drummond Scientific, Broomall, PA). The oocytes were incubated in a solution containing 96-mM NaCl, 2-mM KCl, 1.8-mM CaCl₂, 2-mM MgCl₂, and 5-mM HEPES (pH 7.4), supplemented with 50 mg/l gentamycin sulfate.

Two-electrode voltage-clamp recordings were performed at room temperature (18–22 °C) using a Geneclamp 500 amplifier (Molecular Devices, Downingtown, PA) controlled by a pClamp data acquisition system (Axon Instruments, Union City, CA). Whole cell currents from oocytes were recorded 1–4 days after injection. Bath solution composition was 96-mM NaCl, 2-mM KCl, 1.8-mM CaCl₂, 2-mM MgCl₂, and 5-mM HEPES (pH 7.4). Toxins were applied directly to the bath. Resistances of both electrodes were kept between 0.8 and 1.5 MΩ. The elicited currents were filtered at 1 kHz and sampled at 20 kHz using a four-pole low-pass Bessel filter. Leak subtraction was performed using a -P/4 protocol. Only data obtained from cells exhibiting currents with peak amplitude below 2 µA were considered for analysis. For the electrophysiological analysis of Nv1, Nv4 and Nv5 a number of protocols were applied from a holding potential of −90 mV with a start-to-start interval of 0.2 Hz. Kv1.1–Kv1.6 and Shaker currents were evoked by 250-ms depolarizations to 0 mV followed by a 250 ms pulse to −50 mV from a holding potential of −90 mV. Current traces of hERG channels were elicited by applying a +40 mV prepulse for 2 s followed by a step to −120 mV for 2 s. Kv2.1, Kv3.1, and Kv4.3 currents were elicited by 250 ms pulses to +20 mV from a holding potential of −90 mV. Kv7 and Kv10.1 currents were evoked by 2-s depolarizing pulses to 0 mV from a holding

potential of −90 mV. Sodium current traces were evoked by 100-ms depolarization to the voltage corresponding to maximal sodium current in control conditions. All data were analyzed using pClamp Clampfit 10.0 (Molecular Devices) and Origin 7.5 software (Originlab, Northampton, MA).

Supplementary Material

Supplementary data are available at *Molecular Biology and Evolution* online.

Acknowledgments

The authors are grateful to the following researchers of the core facilities of the Alexander Silberman Institute of Life Sciences, The Hebrew University: Dr William Breuer (Interdepartmental Unit) for his help with mass spectrometry, Dr Mario Lebendiker (Protein Expression and Purification Unit) for his help with chromatography, and Dr Naomi Melamed-Book (Advanced Imaging Unit) for her help with confocal microscopy. This work was supported by Israel Science Foundation grant 869/18 to Y.M. and United States-Israel Binational Science Foundation grant 2014667 to Y.M. in collaboration with A.M.R. Members of the Reitzel lab at UNC Charlotte (A.M.R. and J.M.) were supported by National Science Foundation award #1536530.

References

- Anderluh G, Podlessek Z, Macek P. 2000. A common motif in proteins of Cnidarian toxins and nematocyst collagens and its putative role. *Biochim Biophys Acta* 1476(2):372–376.
- Casewell NR. 2016. Venom evolution: gene loss shapes phenotypic adaptation. *Curr Biol* 26(18):R849–R851.
- Casewell NR, Wuster W, Vonk FJ, Harrison RA, Fry BG. 2013. Complex cocktails: the evolutionary novelty of venoms. *Trends Ecol Evol (Amst)* 28(4):219–229.
- Chen S, Ni X, Krinsky BH, Zhang YE, Vrananovski MD, White KP, Long M. 2012. Reshaping of global gene expression networks and sex-biased gene expression by integration of a young gene. *EMBO J* 31(12):2798–2809.
- Chijiwa T, Deshimaru M, Nobuhisa I, Nakai M, Ogawa T, Oda N, Nakashima K, Fukumaki Y, Shimohigashi Y, Hattori S, et al. 2000. Regional evolution of venom-gland phospholipase A2 isoenzymes of *Trimeresurus flavoviridis* snakes in the southwestern islands of Japan. *Biochem J* 347(Pt 2):491–499.
- Columbus-Shenkar YY, Sachkova MY, Macrander J, Fridrich A, Modepalli V, Reitzel AM, Sunagar K, Moran Y. 2018. Dynamics of venom composition across a complex life cycle. *eLife* 7: pii: e35014.
- Darling JA, Reitzel AR, Burton PM, Mazza ME, Ryan JF, Sullivan JC, Finnerty JR. 2005. Rising starlet: the starlet sea anemone, *Nematostella vectensis*. *BioEssays* 27(2):211–221.
- Darriba D, Taboada GL, Doallo R, Posada D. 2011. ProtTest 3: fast selection of best-fit models of protein evolution. *Bioinformatics* 27(8):1164–1165.
- Dowell NL, Giorgianni MW, Kassner VA, Selegue JE, Sanchez EE, Carroll SB. 2016. The deep origin and recent loss of venom toxin genes in rattlesnakes. *Curr Biol* 26(18):2434–2445.
- Dutertre S, Jin A-H, Vetter I, Hamilton B, Sunagar K, Lavergne V, Dutertre V, Fry BG, Antunes A, Venter DJ, et al. 2014. Evolution of separate predation- and defence-evoked venoms in carnivorous cone snails. *Nat Commun* 5:3521.
- Eickbush TH, Eickbush DG. 2007. Finely orchestrated movements: evolution of the ribosomal RNA genes. *Genetics* 175(2):477–485.

- Fischer AH, Mozzherin D, Eren AM, Lans KD, Wilson N, Cosentino C, Smith J. 2014. SeaBase: a multispecies transcriptomic resource and platform for gene network inference. *Integr Comp Biol*. 54(2):250–263.
- Frank P, Bleakney J. 1978. Asexual reproduction, diet, and anomalies of the anemone *Nematostella vectensis* in Nova Scotia. *Can Field Nat*. 92:259–263.
- Frickey T, Lupas A. 2004. CLANS: a Java application for visualizing protein families based on pairwise similarity. *Bioinformatics* 20(18):3702–3704.
- Fry BG, Wuster W, Kini RM, Brusic V, Khan A, Venkataraman D, Rooney AP. 2003. Molecular evolution and phylogeny of elapid snake venom three-finger toxins. *J Mol Evol*. 57(1):110–129.
- Genikhovich G, Technau U. 2009. Induction of spawning in the starlet sea anemone *Nematostella vectensis*, in vitro fertilization of gametes, and dejellying of zygotes. *Cold Spring Harb Protoc*. 2009: pdb.prot5281.
- Gouy M, Guindon S, Gascuel O. 2010. SeaView version 4: a multiplatform graphical user interface for sequence alignment and phylogenetic tree building. *Mol Biol Evol*. 27(2):221–224.
- Guindon S, Dufayard JF, Lefort V, Anisimova M, Hordijk W, Gascuel O. 2010. New algorithms and methods to estimate maximum-likelihood phylogenies: assessing the performance of PhyML 3.0. *Syst Biol*. 59(3):307–321.
- Hand C, Uhlinger KR. 1992. The culture, sexual and asexual reproduction, and growth of the sea anemone *Nematostella vectensis*. *Biol Bull*. 182(2):169–176.
- Hemmrich G, Bosch TC. 2008. Compagen, a comparative genomics platform for early branching metazoan animals, reveals early origins of genes regulating stem-cell differentiation. *BioEssays* 30(10):1010–1018.
- Honma T, Shiomi K. 2006. Peptide toxins in sea anemones: structural and functional aspects. *Mar Biotechnol*. 8(1):1–10.
- Huang Y, Niu B, Gao Y, Fu L, Li W. 2010. CD-HIT Suite: a web server for clustering and comparing biological sequences. *Bioinformatics* 26(5):680–682.
- Jekely G. 2013. Global view of the evolution and diversity of metazoan neuropeptide signaling. *Proc Natl Acad Sci U S A*. 110(21):8702–8707.
- Jouiaei M, Sunagar K, Federman Gross A, Scheib H, Alewood PF, Moran Y, Fry BG. 2015. Evolution of an ancient venom: recognition of a novel family of cnidarian toxins and the common evolutionary origin of sodium and potassium neurotoxins in sea anemone. *Mol Biol Evol*. 32(6):1598–1610.
- Katoh K, Rozewicki J, Yamada KD. 2017. MAFFT online service: multiple sequence alignment, interactive sequence choice and visualization. *Brief Bioinform*. bbx108, <https://doi.org/10.1093/bib/bbx108>
- Keller I, Chintauan-Marquier IC, Veltsos P, Nichols RA. 2006. Ribosomal DNA in the grasshopper *Podisma pedestris*: escape from concerted evolution. *Genetics* 174(2):863–874.
- Kneib R. 1985. Predation and disturbance by grass shrimp, *Palaemonetes pugio* Holthuis, in soft-substratum benthic invertebrate assemblages. *J Exp Mar Biol Ecol*. 93(1-2):91–102.
- Liao D. 1999. Concerted evolution: molecular mechanism and biological implications. *Am J Hum Genet*. 64(1):24–30.
- Liew YJ, Aranda M, Voolstra CR. 2016. Reefgenomics.Org—A Repository for Marine Genomics Data. Database Database, baw152, <https://doi.org/10.1093/database/baw152>
- Logashina YA, Mosharova IV, Korolkova YV, Shelukhina IV, Dyachenko IA, Palikov VA, Palikova YA, Murashev AN, Kozlov SA, Stensvag K, et al. 2017. Peptide from sea anemone *Metridium senile* affects Transient Receptor Potential Ankyrin-repeat 1 (TRPA1) function and produces analgesic effect. *J Biol Chem*. 292(7):2992–3004.
- Macrander J, Broe M, Daly M. 2016. Tissue-specific venom composition and differential gene expression in sea anemones. *Genome Biol Evol*. 8(8):2358–2375.
- Moran Y, Genikhovich G, Gordon D, Wienkoop S, Zenkert C, Ozbek S, Technau U, Gurevitz M. 2012. Neurotoxin localization to ectodermal gland cells uncovers an alternative mechanism of venom delivery in sea anemones. *Proc R Soc B Biol Sci*. 279(1732):1351–1358.
- Moran Y, Gordon D, Gurevitz M. 2009. Sea anemone toxins affecting voltage-gated sodium channels—molecular and evolutionary features. *Toxicon* 54(8):1089–1101.
- Moran Y, Gurevitz M. 2006. When positive selection of neurotoxin genes is missing. The riddle of the sea anemone *Nematostella vectensis*. *FEBS J*. 273(17):3886–3892.
- Moran Y, Praher D, Schlesinger A, Ayalon A, Tal Y, Technau U. 2013. Analysis of soluble protein contents from the nematocysts of a model sea anemone sheds light on venom evolution. *Mar Biotechnol*. 15(3):329–339.
- Moran Y, Weinberger H, Reitzel AM, Sullivan JC, Kahn R, Gordon D, Finnerty JR, Gurevitz M. 2008. Intron retention as a posttranscriptional regulatory mechanism of neurotoxin expression at early life stages of the starlet anemone *Nematostella vectensis*. *J Mol Biol*. 380(3):437–443.
- Moran Y, Weinberger H, Sullivan JC, Reitzel AM, Finnerty JR, Gurevitz M. 2008. Concerted evolution of sea anemone neurotoxin genes is revealed through analysis of the *Nematostella vectensis* genome. *Mol Biol Evol*. 25(4):737–747.
- Mouhat S, Jouirou B, Mosbah A, De Waard M, Sabatier JM. 2004. Diversity of folds in animal toxins acting on ion channels. *Biochem J*. 378(Pt 3):717–726.
- Nei M, Rooney AP. 2005. Concerted and birth-and-death evolution of multigene families. *Annu Rev Genet*. 39:121–152.
- Peigneur S, Cologna CT, Cremonez CM, Mille BG, Pucca MB, Cuypers E, Arantes EC, Tytgat J. 2015. A gamut of undiscovered electrophysiological effects produced by *Tityus serrulatus* toxin 1 on NaV-type isoforms. *Neuropharmacology* 95:269–277.
- Petersen TN, Brunak S, von Heijne G, Nielsen H. 2011. SignalP 4.0: discriminating signal peptides from transmembrane regions. *Nat Methods*. 8(10):785–786.
- Putnam NH, Srivastava M, Hellsten U, Dirks B, Chapman J, Salamov A, Terry A, Shapiro H, Lindquist E, Kapitonov VV, et al. 2007. Sea anemone genome reveals ancestral eumetazoan gene repertoire and genomic organization. *Science* 317(5834):86–94.
- Renfer E, Technau U. 2017. Meganuclease-assisted generation of stable transgenics in the sea anemone *Nematostella vectensis*. *Nat Protoc*. 12(9):1844–1854.
- Rodriguez E, Barbeitos MS, Brugler MR, Crowley LM, Grajales A, Gusmao L, Haussermann V, Reft A, Daly M. 2014. Hidden among sea anemones: the first comprehensive phylogenetic reconstruction of the order Actiniaria (Cnidaria, Anthozoa, Hexacorallia) reveals a novel group of hexacorals. *PLoS One* 9(5):e96998.
- Ronquist F, Teslenko M, van der Mark P, Ayres DL, Darling A, Höhna S, Larget B, Liu L, Suchard MA, Huelsenbeck JP. 2012. MrBayes 3.2: efficient Bayesian phylogenetic inference and model choice across a large model space. *Syst Biol*. 61(3):539–542.
- Sebe-Pedros A, Saudemont B, Chomsky E, Plessier F, Mailhe MP, Renno J, Loe-Mie Y, Lifshitz A, Mukamel Z, Schmutz S, et al. 2018. Cnidarian cell type diversity and regulation revealed by whole-organism single-cell RNA-Seq. *Cell* 173:1520–1534 e1520.
- Shaner NC, Lin MZ, McKeown MR, Steinbach PA, Hazelwood KL, Davidson MW, Tsien RY. 2008. Improving the photostability of bright monomeric orange and red fluorescent proteins. *Nat Methods*. 5(6):545–551.
- Stefanik DJ, Lubinski TJ, Granger BR, Byrd AL, Reitzel AM, DeFilippo L, Lorenc A, Finnerty JR. 2014. Production of a reference transcriptome and transcriptomic database (EdwardsiellaBase) for the lined sea anemone, *Edwardsiella lineata*, a parasitic cnidarian. *BMC Genomics*. 15:71.
- Sugino RP, Innan H. 2006. Selection for more of the same product as a force to enhance concerted evolution of duplicated genes. *Trends Genet*. 22(12):642–644.
- Surm JM, Smith HL, Madio B, Undheim EAB, King GF, Hamilton BR, van der Burg CA, Pavasovic A, Prentis PJ. Forthcoming 2019. A process of convergent amplification and tissue-specific expression dominate

- the evolution of toxin and toxin-like genes in sea anemones. *Mol Ecol*. 00: 1– 18. <https://doi.org/10.1111/mec.15084>
- Walker AA, Mayhew ML, Jin J, Herzig V, Undheim EAB, Sombke A, Fry BG, Meritt DJ, King GF. 2018. The assassin bug *Pristhesancus plagipennis* produces two distinct venoms in separate gland lumens. *Nat Commun*. 9(1):755.
- Wang S, Chen Y. 2018. Phylogenomic analysis demonstrates a pattern of rare and long-lasting concerted evolution in prokaryotes. *Commun Biol*. 1:12.
- Warner JF, Guerlais V, Amiel AR, Johnston H, Nedoncelle K, Rottinger E. 2018. NvERTx: a gene expression database to compare embryogenesis and regeneration in the sea anemone *Nematostella vectensis*. *Development* 145: pii: dev162867.
- Zhang J, Zhang YP, Rosenberg HF. 2002. Adaptive evolution of a duplicated pancreatic ribonuclease gene in a leaf-eating monkey. *Nat Genet*. 30(4):411–415.